



17th International Conference on Greenhouse Gas Control Technologies, GHGT-17

20th -24th October 2024 Calgary, Canada

Techno-economic comparison of blue and turquoise hydrogen production technologies

Alessandro de Cataldo*, Paolo Colbertaldo, Stefano Campanari, Matteo C. Romano

Politecnico di Milano, Department of Energy, via Lambruschini 4, 20156, Milano, Italy

Abstract

The objective of this work is to analyze and compare systems for the production of low-carbon hydrogen from natural gas through methane pyrolysis. An electrically heated methane pyrolysis (MP) plant is modelled and compared with SMR-based technologies as (i) an advanced ultra-low emission blue hydrogen plant based on a Fired Tubular Reformer (FTR-Plus) and (ii) an Auto-thermal Reformer (ATR) with pre-combustion Carbon Capture. The plants were modeled and studied from a techno-economic perspective. The MP plant exhibits a conversion efficiency of 57.7%, compared to 71.3% for FTR-Plus and 73.6% for ATR, and captures 95.8% of CO₂ as solid carbon, against 90.5% and 94.1% for FTR-Plus and ATR, respectively. The MP plant shows a Levelized Cost of Hydrogen (LCOH) of 3.4 €/kg for a capacity of 30 MW_{H₂, LHV}, with a natural gas price of 6 €/GJ_{NG, LHV} and electricity price of 60 €/MWh_e. A sensitivity analysis is conducted to highlight the factors most influencing costs. Finally, the LCOH is compared with SMR-based plant costs for different capacities, considering CO₂ transport via pipeline or truck. The MP plant proves competitive, particularly if carbon is economically valorized, for small to medium capacities due to the reduced capital expenditures and the absence of costs connected to CO₂ transportation.

Keywords: Natural gas, Methane Pyrolysis, Carbon Capture and Storage, Blue Hydrogen, Turquoise Hydrogen

1. Introduction

Low-carbon hydrogen production from natural gas with carbon capture and storage is poised to play a crucial role in reducing industrial emissions. Alongside conventional blue hydrogen methods such as Steam Methane Reforming (SMR), methane pyrolysis (MP) is increasingly recognized as a promising low-carbon technology for producing hydrogen from both fossil and renewable gas sources [1–4]. Although the process has been extensively studied, past interest in MP was largely motivated by the production of carbon black [5]. Recently, several companies have adopted plasma-based pyrolysis (i.e., methane splitting through plasma interaction); among them, Monolith Materials is the only company currently operating a demonstrative MP plant, producing 5 kt of hydrogen annually as a by-product, with carbon black being the primary output of the process [6,7]. This study focuses on thermo-catalytic methane decomposition to produce hydrogen, using supported metal catalysts.

* Corresponding author. Email address: alessandro.decataldo@polimi.it

Nomenclature

ASU	Air separation unit
ATR	Auto-thermal reformer
CCS	Carbon capture and storage
CCR	Carbon capture ratio
CGE	Cold gas efficiency
LCOH	Levelized cost of hydrogen
LHV	Lower heating value
FTR	Fired tubular reformer
ICC	Inter-cooled compressor
IRR	Internal rate of return
KPI	Key performance indicators
MDEA	Methyl diethanolamine
MP	Methane pyrolysis
NG	Natural gas
PSA	Pressure swing adsorber
S/C	Steam to carbon ratio
SC	Steam cycle
SMR	Steam methane reforming
WGS	Water gas shift

Several experimental studies on methane pyrolysis with iron and nickel-based catalysts in different reactors, such as fixed beds [8], fluidized beds [9–13], and rotary beds [14,15], have demonstrated that reaction can obtain stable conditions and approach equilibrium. However, carbon deposition leading to catalyst deactivation remains a challenge. Various catalysts, from carbon-based to metal-based, operate across different space velocities, temperatures, and pressures, producing a wide range of carbon species [16], from amorphous carbon to valuable carbon nanotubes and nanofibers (single-walled and multi-walled) [11]. These byproducts differ in density [10,17], carbon content, and economic value [18].

This paper aims to:

- conduct a techno-economic analysis of the MP process, assessing mass and energy balances and economic Key Performance Indicators (KPIs);
- compare alternative low-carbon hydrogen production processes based on methane pyrolysis (turquoise hydrogen) and steam methane reforming with CCS (blue hydrogen).

Additionally, the study will explore:

- technology improvements and operational parameters for decarbonizing hydrogen production at various scales
- different economic frameworks and scenarios for profitable use of blue and turquoise hydrogen technologies.

2. Plant description

The plant scheme is shown in Figure 1. The input gas, whether fossil-based or renewable, first undergoes purification in a high-pressure, low-temperature desulfurization section using activated carbon [19]. After this, the gas is throttled before entering the pyrolysis section. In the pyrolysis reactor, the feedstock is heated by a counter-flow moving bed, which is in contact with the carbon-loaded catalyst exiting the reactor. The solid catalyst feed, introduced from the top of the reactor, is preheated in a counter-flow moving bed against the hydrogen-rich pyrogas. The reactor's reaction section is electrically heated to reach the necessary temperature and supply the reaction heat. The pyrogas produced is cooled and directed to an inter-cooled compressor (ICC) before being sent to a hydrogen purification section, utilizing a Pressure Swing Adsorption (PSA) unit. A portion of the unconverted methane, along with N₂, CO, H₂O, and CO₂ (the latter due to the CO₂ in the inlet gas), from the PSA off-gas is recirculated back to the pyrolysis reactor to improve overall methane conversion. The recirculated stream is preheated by cooling the pyrogas leaving the

reactor. The remaining purge gas is removed from the plant and combusted. The loaded catalyst is sent to storage, regeneration or recycle with separation of solid carbon, which could be potentially sold for specific market uses (e.g. consumption in the production of tyres, inks..).

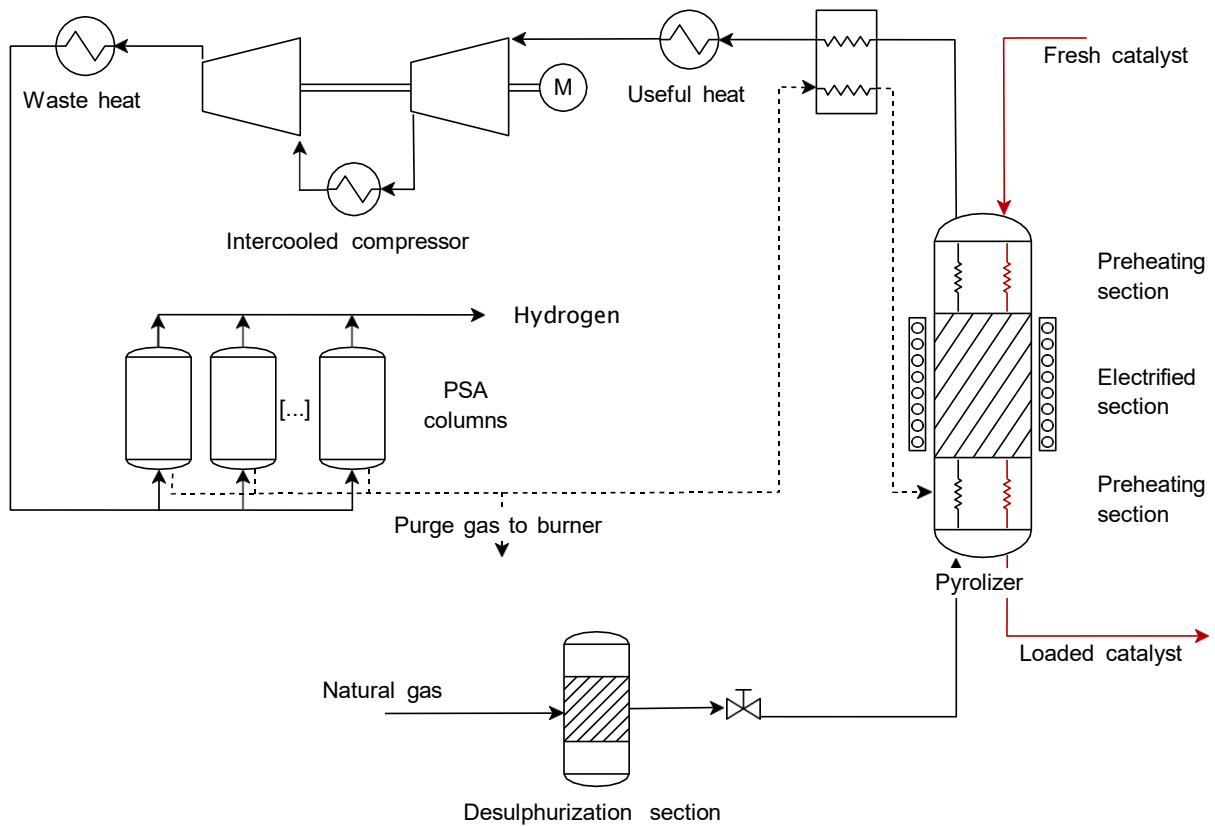


Figure 1 – Block flow diagram of the MP plant

2.1. Method

The energy and mass balances of the plants are evaluated using Aspen Plus, employing the Peng-Robinson Equation-of-State with Boston-Mathias modification (PR-BM) property method [20,21]. All the reactions involved are assumed to reach chemical equilibrium. The primary reactions taking place in the MP reactor are the pyrolysis of methane and other hydrocarbons. Secondary reactions, namely steam methane reforming, dry reforming, water gas shift and carbon gasification are induced by the oxygen carried by the CO_2 contained in the feedstock. It is assumed that for the considered range of temperature and pressure, the other hydrocarbons are fully cracked [22]. This study evaluates an iron-based catalysts, which achieve carbon loadings in the ranges of 2-5 gC/g_{cat} [23], including the related supply cost in the economic analysis. Depending on the quality of the solid carbon two options would be considered regarding (i) the revenues associated with economic valorization and (ii) the negative costs incurred by solid carbon disposal. Table 1 shows the main assumptions of this study. The MP plant is sized to convert 52 MW_{LHV} of natural gas, producing 30 MW_{LHV} (or 10'086 Nm^3/h) of high purity hydrogen.

2.2. Benchmarking technologies

The following low-carbon hydrogen benchmark technologies are considered for comparison with the MP plant:

- Fired Tubular reformer (FTR-Plus) case: this case involves hydrogen production using a Fired Tubular Reformer with CO_2 capture. The plant features a specific process configuration and advanced operational

parameters, such as an H₂-fired FTR furnace, higher reforming temperatures, high-efficiency CO₂ separation, and an isothermal low-temperature water-gas shift reactor. This setup allows for a CO₂ capture efficiency of over 90%, relying solely on pre-combustion CO₂ separation.

- Auto-thermal reformer (ATR) case: this case focuses on hydrogen production in an Auto-Thermal Reformer (ATR), which consists of a refractory vessel where a portion of the feedstock is oxidized under sub-stoichiometric conditions to sustain the reaction. The reactor operates at a temperature of 1050°C, with air supplied through an Air Separation Unit (ASU). The high operating temperature and the partial oxidation of methane lead to a higher CO₂ concentration in the syngas, resulting in an overall greater carbon capture ratio (CCR) compared to an FTR.

Both the ATR and FTR-Plus plants have been extensively characterized by some authors of this paper in [24], and are designed to produce low-carbon blue hydrogen with a carbon capture ratio ranging from 90% to 95%.

Table 1 – Main assumptions for the calculation of the mass and energy balances of the MP plant

Component	Main assumption
Pyrolysis plant	
Natural gas	
Input flow rate	5245 Nm ³ /h (52 MW _{LHV})
Composition	CH ₄ :89%/C ₂ H ₆ :7%/C ₃ H ₈ :1%/C ₄ H ₁₀ :0.1%/C ₅ H ₁₂ :0.01%/CO ₂ :0.89%/N ₂ :2%
MP reactor	
Reactor temperature	800 °C
Reactor pressure	1 bar
Preheating sections	
Solid-gas ΔT _{min}	5°C
Pressure loss	1 bar
PSA off-gas preheater	
Off-gas recycle ratio to reactor	87.4%
Pinch point ΔT	25°C
Off-gas outlet temperature	400°C
PSA unit	
Hydrogen purity	99.99+%
H ₂ separation efficiency	95%
Pyrogas Compressor (Intercooled)	
Outlet pressure	30 bar
Intercooling temperature	40°C
Isentropic efficiency	85%
Mechanical-electric efficiency	98%

2.3. Key Performance Indicators (KPIs)

The selected technologies are compared accordingly with the following KPIs:

- Cold-Gas Efficiency (CGE), defined as the ratio between the chemical LHV energy output of pure H₂ and the NG input (Eq. (1)).

- CGE*, defined as the ratio between the chemical LHV energy output over the NG input, the total net electric consumption and the heat production (considering heat to be alternatively produced by burning NG in a boiler with 90% efficiency) (Eq. (2)).
- Carbon Capture Ratio (CCR): defined as the ratio between the moles of carbon leaving as solid carbon and the moles of atomic carbon entering with natural gas (Eq. (3)).

$$CGE = \frac{\dot{m}_{out} LHV_{out}}{\dot{m}_{NG} LHV_{NG}} \quad \text{Eq. (1)}$$

$$CGE^* = \frac{\dot{m}_{out} LHV_{out}}{\dot{m}_{NG} LHV_{NG} + P_{el,consumption} - \frac{P_{th,produced}}{\eta_{boiler}}} \quad \text{Eq. (2)}$$

$$CCR = \frac{\dot{n}_{C,solid,out}}{\dot{n}_{C,NG,in}} \quad \text{Eq. (3)}$$

3. Results

The Sankey diagrams for the energy and carbon balances of the MP plant are shown in Figure 2. The energy Sankey diagram refers to a natural gas input of 100 units of energy on LHV basis. The exported hydrogen is 57.7 MJ/100MJ_{NG}, while the solid carbon output accounts for 48.8 MJ/100MJ_{NG}. The pyrogas is cooled down, allowing to recover 5.5 MJ_{th}/100MJ_{NG} of medium-high temperature heat (above 150 °C) and rejecting 0.7 MJ_{th}/100MJ_{NG} as low-temperature heat. The IC pyrogas compressor consumes 4.2 MJ_e/100MJ_{NG} and exchanges 4.2 MJ_{th}/100MJ_{NG} with the cooling media. Of the PSA off gas, a stream equivalent to 17.7 MJ/100MJ_{NG} is recirculated to the MP reactor and the remaining part (corresponding to 2.5 MJ/100MJ_{NG}) is exported to an off-gas burner. The MP reactor electric heater consumes 15.4 MJ_e/100MJ_{NG}. Overall, in addition to H₂, the plant can deliver 7.80 MJ_{th}/100MJ_{NG} of high-quality heat from pyrogas cooling and PSA off-gas combustion. The carbon Sankey diagram is scaled on 100 moles of carbon entering the system with natural gas. Of this, 95.6 moles leave the system as solid carbon, while the remainder leaves as unconverted CH₄, CO, and CO₂, in the purged PSA off-gas. The recirculated PSA off-gas contains 29.2 moles of carbon, primarily CO.

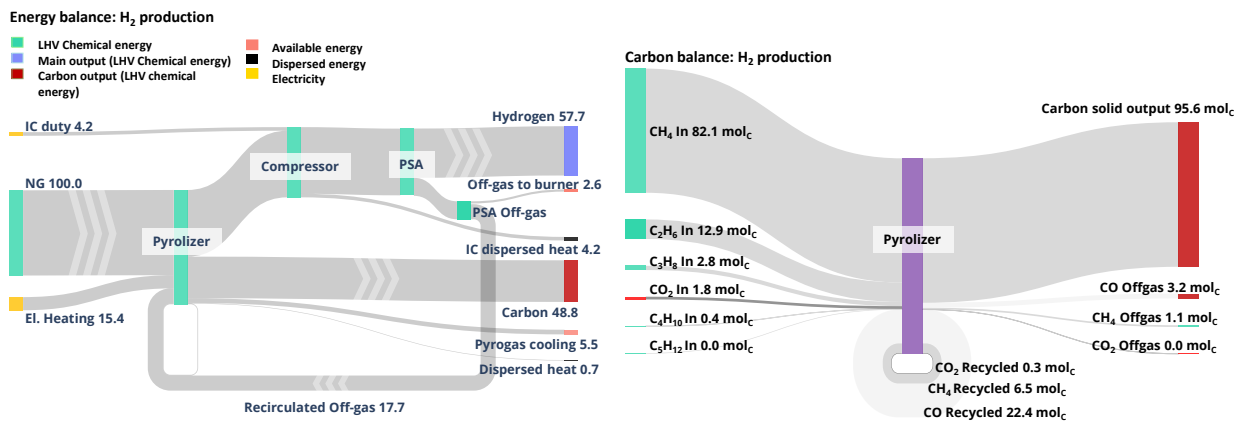


Figure 2 - Sankey diagram of the MP plant for the energy balance, referred to 100 unit of LHV energy of inlet NG (top), and carbon balance, referred to 100 moles of inlet carbon (bottom).

Table 2 details the heat and mass balances and the performances for MP technologies and the two benchmark SMR-based plants, all scaled to a reference size of 30 MW of exported H₂ (corresponding to about 10'086 Nm³/h). The CGE of the MP plants is lower than that of the FTR-Plus (71.3%) and ATR (73.6%) plants. This can be explained

from the stoichiometry of the reactions, leading to maximum theoretical CGE of 60% (i.e. 2 mol_{H2}/mol_{CH4}) for MP and 120% (i.e. 4 mol_{H2}/mol_{CH4}) for SMR+WGS reactions. For the SMR-based plants, two different values for specific net electric output are provided. The first case considers the separation and compression of CO₂ to pipeline conditions (110 bar). The second case, however, involves compressing and liquefying the produced CO₂. In this alternative scenario, a specific energy consumption of 132 kWh/t_{CO2} is assumed, as noted in [25].

Table 2 – Performance of MP and SMR-based plants

	MP	FTR-Plus	ATR
NG thermal input, MW _{LHV}	51.99	42.05	40.78
Hydrogen output, MW _{LHV}	30.00	30.00	30.00
Hydrogen output, Nm ³ /h	10'086	10'086	10'086
Net electric output, MW _{el}	-10.19	0.86	0.57
Carbon output, MW _{LHV}	24.37	-	-
Useful heat, MW _{th}	4.04	-	-
Specific net electric output, kWh/kg _{H2}	-11.32	0.952 / 0.637 ^b	0.632 / 0.303 ^b
CGE, %	57.70	71.33	73.57
CGE*, %	52.00	72.83	74.61
Carbon capture ratio, %	95.80	90.52	94.13
Specific direct emission g _{CO2} /MJ _{H2}	4.15	7.58	4.55
Specific direct emission kg _{CO2} /kg _{H2}	0.50	0.91	0.55

^a values refer to the electricity net output if a cryogenic liquefaction section is considered instead of the conventional CO₂ compression section

4. Economic analysis

The economic analysis was conducted aiming at determining which technology allows for the lowest Levelized Cost of Hydrogen (LCOH). The study is based on Discounted Cash Flow analysis. Depreciation was not considered, since the results are reported on the Earnings Before Interest, Taxes, Depreciation and Amortization (EBITDA) basis according to procedure described in [26]. Table 3 shows the assumed financial parameters for the economic analysis.

Table 3 – Main parameters for the economic analysis

Euro valued in year	2023
Construction period	3 years
Capital expenditure curve	20/45/35% (1st ,2nd,3rd year)
Interest during construction	8%
Number of hydrogen plants	10
Plants lifetime	25 years
Capacity factor	91% (8000 equivalent hours)
Discount rate	8%
Owner's cost	7%

4.1. Capital cost estimation

The Total Plant Cost (TPC) is evaluated by scaling the reference values given in [27] scaled for considered size and updated to €2023 via the Chemical Engineering Plant Cost Index (CEPCI). Reference cost includes Equipment and Material costs, Manufacturing costs and Process and project contingencies & Engineering Fees. The cost for the reactor is taken from previous literature studies by Keipi et al. [28] for a similar electrified reactor with two direct

contact heat recovery sections. The Total capital requirement (TCR) is then calculated considering startup costs, spare part costs, owner's cost, interest during construction and working capital as described in [26]. Table 4 shows the cost breakdown for both the MP plant and for the SMR-based plants for the specific size selected for the study, evaluated consistently with previous works from some of the authors of this paper [24].

Table 4 – Capex breakdown for the MP and SMR-based plants

H ₂ capacity: 30 MW – 10'086 Nm ³ /h	MP		FTR-Plus		ATR	
	[M€]	[%]	[M€]	[%]	[M€]	[%]
Air separation unit					36.40	36.7%
Syngas generation	21.23	43.8%	26.46	33.8%	14.21	14.3%
CO ₂ separation and compression			16.43 – 16.81 ^a	21.0%	15.29- 15.68 ^a	15.4%
Hydrogen purification	3.97	8.2%	5.77	7.4%	5.77	5.8%
Steam cycle, Feedwater and Miscellaneous BOP Systems ^b	23.31	48.1%	29.53	37.8%	27.48	27.7%
Total plant cost M€	48.5		78.2		99.2	
Specific TPC €/kW _{H₂-exp}	1617.1		2608		3307	
Total capital requirements, M€	62.6		100.3		127.0	

^a these values consider the alternative of liquefying CO₂ for truck transportation instead of compressing CO₂ for pipeline transportation

^b no steam cycle, or feedwater system for the MP case

4.2. Operating costs estimation

The fixed operating costs include annual maintenance cost (1.5% of TPC), direct labor cost (83'000 € with variable number of personnel) administrative and support labor cost (30 % of the direct labor plus the maintenance labor cost assumed as 40 % of the overall maintenance cost). The number of personnel has been determined in accordance with the IEAGHG report [26] and is 21, 23, and 25 for MP, FTR-Plus, and ATR, respectively. This number increases with the complexity and scale of the plant. Table 5 shows the unit costs for the main consumables (NG feedstock, electricity, catalyst, carbon management) and for stored, transported and emitted CO₂. As no carbon valorization is assumed for the baseline case the analysis considered both the cost for supply and disposal of the produced carbon. The high temperature heat produced by the MP plant is valorized based on the saved natural gas in existing 90%_{LHV} efficient boilers. For the MP case, it is assumed that no revenue is associated with the produced carbon, but the loaded catalyst is sent to disposal. The cost of CO₂ transport for the benchmark SMR plants is computed according to [29], assuming pipeline transport over a distance of 200 km, unit costs depending on the pipeline capacity, as reported in Table 5. For limited quantities of captured CO₂, road transport may be a more viable option, costs for truck transport are adapted from [30].

The Levelized Cost of Hydrogen (LCOH) has been evaluated using a first-year approach, i.e. the values refer to the cost of the first year of production. The distribution of LCOH for MP and SMR based plants is shown in Figure 3 and exhibits several notable differences. For both MP and SMR based plants the cost of natural gas is the most impacting factor at the largest capacity. Due to the unfavorable stoichiometry MP plants entail higher feedstock consumption and thus higher cost. Catalyst consumption is significantly higher in MP-based plants compared to SMR-based plants: this is due to the very limited time on stream for the selected catalyst, which experiences a rapid decline in activity associated with carbon accumulation and must be discharged after a relatively short operation, the presented cost already includes cost of carbon disposal. While ATR and FTR-Plus are net electricity exporters, the electric consumption from MP plant is significant (11.4 kWh/kg_{H₂}) and thus it is the impact of the cost of electricity on the final cost. The CO₂ transport and storage cost is absent for MP plants. The graph evaluates two different plant sizes, ranging from medium-small to large scale. As the plant size decreases, the necessity for a shared pipeline arises and CO₂ Transport cost increases significantly. Passing from 300MW to 30MW truck transport of liquified CO₂ becomes

more competitive and it is thus considered in the chart as a preferred option over pipeline transportation. Finally, as the scale of the plant is reduced the impact of the cost of the personnel increases considerably since staff members are decreasing less than proportionally with respect to size.

Table 5 – Assumptions on consumables and operating costs

Variable costs	Unit	Cost
Natural gas	€/GJ _{LHV}	6
Electricity selling/purchasing price	€/MWh _{el}	60
CO ₂ storage cost	€/t _{CO2} stored	10
CO ₂ transport cost (pipeline) [29]	€/km/t _{CO2} transported	0.102x ^{-0.36} where x is the transported CO ₂ in Mt/y ^a
CO ₂ transport cost (liquid CO ₂)	€/km	2.30 ^b
CO ₂ emission cost	€/t _{CO2} emitted	100
Carbon management cost	€/t _c produced	0 (no valorization of solid carbon)
Iron catalyst cost	€/t _{cat} fresh	500
Catalyst disposal cost	€/t _{cat} spent	50
Carbon catalyst loading	g _c /g _{cat}	5
Value of recovered heat	€/MWh	24 ^c

^a cost refers to dense-phase CO₂ transport, updated to 2023

^b the selected specific cost was adapted from a detailed analysis that considers fixed (including investment) and variable costs (including fuel, staff, investment, maintenance [30]).

^c priced as the saved NG combustion in a boiler with 90% thermal efficiency

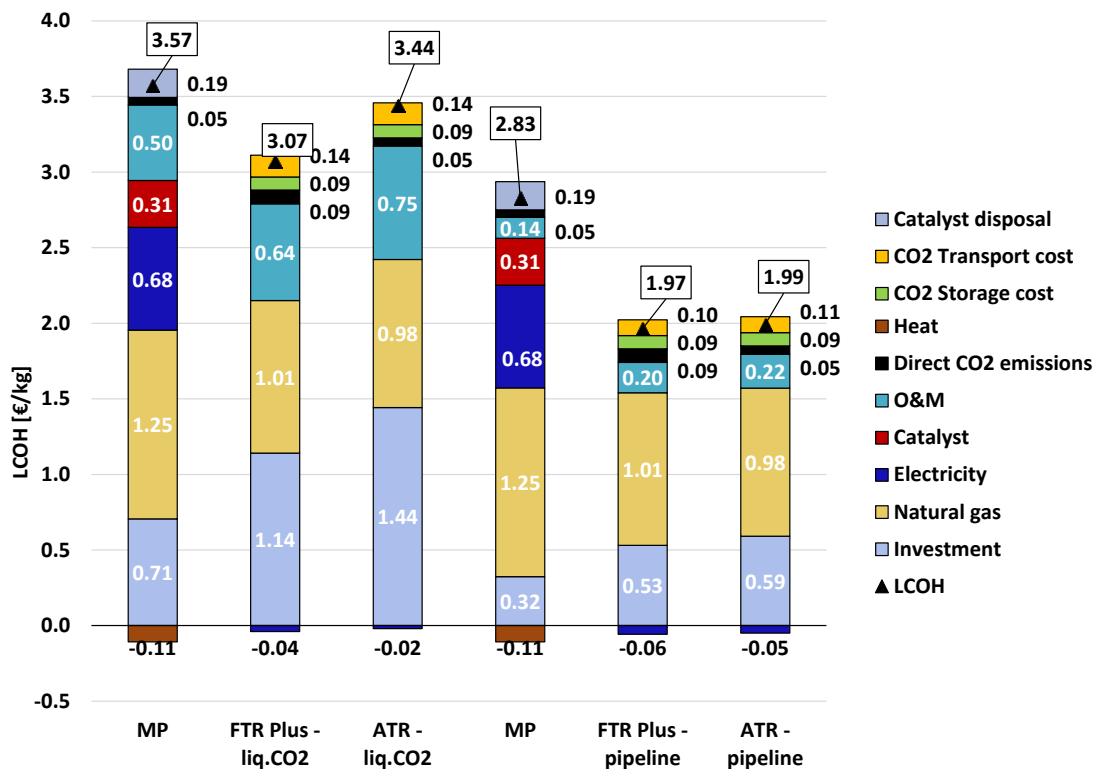


Figure 3 –LCOH for SMR and MP-based plants for 10⁸6 and 100⁸64 Nm³/h plant size

Figure 4 shows the LCOH for the different technologies considering: (i) different CO₂ and carbon transport distances (200 and 700 km); (ii) different valorization of solid carbon (between -50 and 200 €/t); (iii) different hydrogen plant capacities (30 and 300 MW). SMR-based plants show generally lower LCOH at large and medium-small scale, for short CO₂ transport distances. If distance increases to 700 km and scale is reduced, the MP-based plants gain competitiveness. For medium-small scale CO₂ from SMR-based plants is transported in liquid state with trucks as it has been proven to be more competitive. At this scale MP technology is competitive, and particularly when carbon is economically valued. The estimated costs range from 2.8 – 3.6 €/kg_{H₂}. FTR-Plus plants become particularly competitive for short CO₂ transport distances, with costs between 3.1 - 3.4 €/kg. For the base case at large scale, MP technology is only competitive when carbon valorization is high (approximately 0.2 €/kg). Otherwise, the most competitive technologies are SMR-based plants, which are viable for both short and long CO₂ transport distances, with costs ranging from 2.0 to 2.3 €/kg.

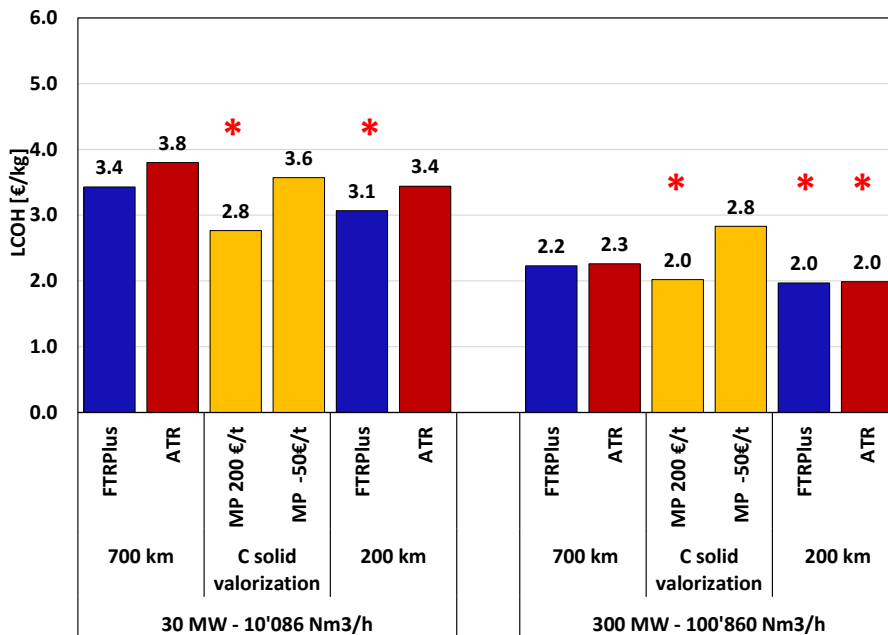


Figure 4 – LCOH for SMR and MP-based plant as a function of H₂ plant capacity and distance from the CO₂ storage site (FTR and ATR) or solid carbon valorization (MP); no CO₂ is transported from the MP plant. Asterisks mark the most competitive technologies

5. Conclusions

The study highlighted that:

- MP-based technologies enable the production of low-carbon hydrogen without requiring a CCS section, allowing for the separation of over 95% of total carbon from the exported gaseous hydrogen in the form of solid carbon, which facilitates transportation.
- MP-based plants for hydrogen production can obtain LCOH in the range 2.0 – 3.6 €/kg; this cost is highly affected by (i) the variable cost of feedstocks (natural gas), electricity and consumables (mainly the catalyst) and (ii) the H₂ production capacity.
- MP plants may be more competitive than SMR-based plants for small-scale hydrogen production due to (i) lower specific plant capital expenditures (CAPEX) and (ii) the elimination of CO₂ transport costs, which are significantly influenced by scale and distance. This advantage is especially pronounced for medium-scale plants that would otherwise need a dedicated CO₂ pipeline or a CO₂ liquefaction section for subsequent transportation by truck.

Bibliography

- [1] Muradov NZ, Veziroğlu TN. From hydrocarbon to hydrogen–carbon to hydrogen economy. *Int J Hydrogen Energy* 2005;30:225–37. <https://doi.org/10.1016/J.IJHYDENE.2004.03.033>.
- [2] Hermesmann M, Müller TE. Green, Turquoise, Blue, or Grey? Environmentally friendly Hydrogen Production in Transforming Energy Systems. *Prog Energy Combust Sci* 2022;90. <https://doi.org/10.1016/j.pecs.2022.100996>.
- [3] Parkinson B, Balcombe P, Speirs JF, Hawkes AD, Hellgardt K. Levelized cost of CO2 mitigation from hydrogen production routes. *Energy Environ Sci* 2019;12:19–40. <https://doi.org/10.1039/c8ee02079e>.
- [4] Diab J, Fulcheri L, Hessel V, Rohani V, Frenklach M. Why turquoise hydrogen will Be a game changer for the energy transition. *Int J Hydrogen Energy* 2022;47:25831–48. <https://doi.org/10.1016/J.IJHYDENE.2022.05.299>.
- [5] Donnet J-B, Bansal RC, Wang M-J. Carbon black : science and technology. Dekker; 1993.
- [6] Jenkins S, Fromm C. Commercial Progress on Turquoise Hydrogen. *Chemical Engineering* n.d. <https://www.chemengonline.com/fullscreen/commercial-progress-on-turquoise-hydrogen/> (accessed July 11, 2024).
- [7] Monolith. Monolith materials: facilities n.d. <https://monolith-corp.com/facilities> (accessed July 11, 2024).
- [8] Suelves I, Pinilla JL, Lázaro MJ, Moliner R, Palacios JM. Effects of reaction conditions on hydrogen production and carbon nanofiber properties generated by methane decomposition in a fixed bed reactor using a NiCuAl catalyst. *J Power Sources* 2009;192:35–42. <https://doi.org/10.1016/j.jpowsour.2008.11.096>.
- [9] Jang HT, Cha WS. Hydrogen production by the thermocatalytic decomposition of methane in a fluidized bed reactor. *Korean Journal of Chemical Engineering* 2007;24:374–7. <https://doi.org/10.1007/s11814-007-5037-9>.
- [10] Qian JX, Enakonda LR, Wang WJ, Gary D, Del-Gallo P, Basset JM, et al. Optimization of a fluidized bed reactor for methane decomposition over Fe/Al2O3 catalysts: Activity and regeneration studies. *Int J Hydrogen Energy* 2019;44:31700–11. <https://doi.org/10.1016/j.ijhydene.2019.10.058>.
- [11] Pinilla JL, Suelves I, Lázaro MJ, Moliner R, Palacios JM. Parametric study of the decomposition of methane using a NiCu/Al2O3 catalyst in a fluidized bed reactor. *Int J Hydrogen Energy*, vol. 35, 2010, p. 9801–9. <https://doi.org/10.1016/j.ijhydene.2009.10.008>.
- [12] Keller M, Sharma A. Hydrogen Production via Methane Cracking on Dry-Coated Fe/ZrO2 with Support Recycle in a Fluidized Bed Process. *Energy and Fuels* 2021;35:847–55. <https://doi.org/10.1021/acs.energyfuels.0c03287>.
- [13] Pinilla JL, Moliner R, Suelves I, Lázaro MJ, Echegoyen Y, Palacios JM. Production of hydrogen and carbon nanofibers by thermal decomposition of methane using metal catalysts in a fluidized bed reactor. *Int J Hydrogen Energy* 2007;32:4821–9. <https://doi.org/10.1016/j.ijhydene.2007.08.013>.
- [14] Pinilla JL, Utrilla R, Lázaro MJ, Suelves I, Moliner R, Palacios JM. A novel rotary reactor configuration for simultaneous production of hydrogen and carbon nanofibers. *Int J Hydrogen Energy* 2009;34:8016–22. <https://doi.org/10.1016/j.ijhydene.2009.07.057>.
- [15] Pinilla JL, Utrilla R, Lázaro MJ, Moliner R, Suelves I, García AB. Ni- and Fe-based catalysts for hydrogen and carbon nanofilament production by catalytic decomposition of methane in a rotary bed reactor. *Fuel Processing Technology* 2011;92:1480–8. <https://doi.org/10.1016/j.fuproc.2011.03.009>.
- [16] Keipi T, Tolvanen KES, Tolvanen H, Konttinen J. Thermo-catalytic decomposition of methane: The effect of reaction parameters on process design and the utilization possibilities of the produced carbon. *Energy Convers Manag* 2016;126:923–34. <https://doi.org/10.1016/J.ENCONMAN.2016.08.060>.
- [17] Pinilla JL, Lázaro MJ, Suelves I, Moliner R, Palacios JM. Characterization of nanofibrous carbon produced at pilot-scale in a fluidized bed reactor by methane decomposition. *Chemical Engineering Journal* 2010;156:170–6. <https://doi.org/10.1016/j.cej.2009.10.032>.
- [18] Prabowo J, Lai L, Chivers B, Burke D, Dinh AH, Ye L, et al. Solid carbon co-products from hydrogen production by methane pyrolysis: Current understandings and recent progress. *Carbon N Y* 2024;216:118507. <https://doi.org/10.1016/J.CARBON.2023.118507>.
- [19] Ko KJ, Kim H, Cho YH, Kim KM, Lee CH. Desulfurization of ultra-low-concentration H2S in natural gas on Cu-impregnated activated carbon: Characteristics and mechanisms. *Sep Purif Technol* 2023;305:122539. <https://doi.org/10.1016/J.SEPPUR.2022.122539>.
- [20] Peng D-Y, Robinson DB. A New Two-Constant Equation of State. *Industrial & Engineering Chemistry Fundamentals* 1976;15:59–64. <https://doi.org/10.1021/i160057a011>.
- [21] Mathias PM, Copeman TW. Extension of the Peng-Robinson equation of state to complex mixtures: Evaluation of the various forms of the local composition concept. *Fluid Phase Equilib* 1983;13:91–108. [https://doi.org/10.1016/0378-3812\(83\)80084-3](https://doi.org/10.1016/0378-3812(83)80084-3).
- [22] Serban M, Lewis MA, Marshall CL, Doctor RD. Hydrogen Production by Direct Contact Pyrolysis of Natural Gas. *Energy & Fuels* 2003;17:705–13. <https://doi.org/10.1021/ef020271q>.
- [23] Torres D, De Llobet S, Pinilla JL, Lázaro MJ, Suelves I, Moliner R. Hydrogen production by catalytic decomposition of methane using a Fe-based catalyst in a fluidized bed reactor. *Journal of Natural Gas Chemistry* 2012;21:367–73. [https://doi.org/10.1016/S1003-9953\(11\)60378-2](https://doi.org/10.1016/S1003-9953(11)60378-2).
- [24] de Cataldo A, Astolfi M, Chiesa P, Campanari S, Romano MC. Ultra-low emission flexible plants for blue hydrogen and power production, with electrically assisted reformers. *Int J Hydrogen Energy* 2023. <https://doi.org/10.1016/J.IJHYDENE.2023.10.159>.
- [25] Nava A, Remondini D, Campanari S, Romano MC. Carbon-negative “emerald hydrogen” from electrified steam methane reforming of biogas: system integration and optimization. *International Journal of Hydrogen Energy* In Press 2024.
- [26] IEAGHG. Techno - Economic Evaluation of SMR Based Standalone (Merchant) Hydrogen Plant with CCS. Technical Report 2017.
- [27] Lewis E, McNaul S, Jamieson M, Henriksen M, Matthews HS, Walsh L, et al. Comparison of Commercial, State-of-the-Art, Fossil-Based Hydrogen Production Technologies. United States: 2022. <https://doi.org/10.2172/1862910>.

- [28] Keipi T, Hankalin V, Nummelin J, Raiko R. Techno-economic analysis of four concepts for thermal decomposition of methane: Reduction of CO₂ emissions in natural gas combustion. *Energy Convers Manag* 2016;110:1–12. <https://doi.org/10.1016/j.enconman.2015.11.057>.
- [29] Kearns D, Liu H, Consoli C. Technology readiness and cost of CCS. 2021.
- [30] van der Meulen S, Grijspaardt T, Mars W, van der Geest W, Roest-Crollius A, Kiel J. Cost Figures for Freight Transport-final report. Zoetermeer: 2023.